Tropical Built Environment Journal. Volume 14, No. 2, 65-91, 2026 www.tbejournal.com
ISSN: 1118-1790

REMOTE SENSING AND LANDSCAPE METRICS FOR QUANTIFYING URBAN MORPHOLOGICAL TRANSFORMATION IN OWERRI, NIGERIA, 1990–2025

Ndukwe Emmanuel Chiemelu[1] and **Chukwudi Andy Okereke**[2]

[1]Department of Geoinformatics and Surveying, Faculty of Environmental Studies, University of Nigeria, Enugu Campus, Enugu, Nigeria

[2]Department of Surveying and Geoinformatics, Faculty of Environmental Sciences, Imo State University, Owerri, Imo State, Nigeria

*Corresponding Author: andyokereke@gmail.com

ORCID: https://orcid.org/0000-0002-2158-168X

Abstract

Rapid, unplanned urban growth is transforming the built environment of many African secondary cities, yet the fine-grained spatial mechanics of this transformation, how patches of built-up land multiply, merge, and reconfigure over time, remain poorly documented outside a handful of primate cities. This study quantified the morphological transformation of Owerri Urban Area, capital of Imo State, Nigeria, over a 35-year period (1990–2025) using multi-temporal land use/land cover (LULC) classification and landscape-pattern (FRAGSTATS) metrics computed at the class (built-up) and landscape levels. Built-up land expanded from 50.42 km² (9.39%) in 1990 to 244.80 km² (45.61%) of the 536.77 km² study area in 2025, an absolute increase of 194.38 km² (+385.52%) and a compound annual rate of change of +4.61%, occurring mainly at the expense of vegetation (−37.88%) and bare land (−62.17%). Rather than following a simple, monotonic trajectory toward fragmentation, class-level metrics for the built-up class show a four-stage morphological sequence: (i) 1990–2000, patch proliferation and dispersed expansion (number of patches, NP, +85.5%; aggregation index, AI, −10.3%); (ii) 2000–2010, rapid expansion and coalescence (percentage of landscape, PLAND, +156.6%; largest patch index, LPI, +334.5%; AI +21.0%); (iii) 2010–2020, consolidation (NP −29.9% while LPI +91.9% and patch cohesion index, COHESION, rose to 99.80); and (iv) 2020–2025, continued consolidation with limited peripheral reconfiguration (NP −4.2%, LPI +3.4%, ENN_MN −2.9%, AI +0.7%). Landscape-level indices (DIVISION, CONTAG, AI) mirror this non-linear trajectory, falling and then partially recovering rather than declining continuously. These results indicate that Owerri's transformation is better characterised as a diffusion–coalescence–consolidation process with limited late-stage reconfiguration than as continuous fragmentation, a finding consistent with, but empirically distinct from, patterns reported for other African secondary cities such as Enugu, Uyo, Kumasi, and Kampala. The paper discusses the implications of this trajectory for infrastructure planning, development control, and peri-urban land management in rapidly growing Nigerian cities, and situates Owerri's experience within the broader literature on urban morphology and landscape ecology.

Keywords: Urban morphology; Landscape metrics; FRAGSTATS; Urban fragmentation; Urban coalescence

1.0 Introduction

1.1 Urban morphology and spatial transformation

Urban morphology is concerned with the built form of cities and seeks to explain the layout and spatial composition of urban structures and open spaces in light of the forces that create, expand, diversify, and transform them (Noaime & Alnaim, 2025). The Conzenian tradition, developed through the detailed town-plan analysis of British towns such as Alnwick, decomposed urban form into three interacting elements (the street system, the plot pattern, and the building fabric) and treated the resulting townscape as a historically layered palimpsest that could be read to reveal successive phases of growth and redevelopment (Whitehand et al., 2009). While this tradition originated in the study of historic European towns, its central premise that urban form is not a static outcome but an evolving product of continuous morphogenetic processes, travels well to the very different context of rapidly urbanising African cities, where the physical fabric is being written and rewritten within a single human generation rather than across centuries. In cities such as Owerri, morphological change is not confined to the redevelopment of existing plots; it is dominated by the wholesale conversion of vegetation, bare land, and agricultural land into new built-up patches, and by the subsequent merging, thickening, and reorganisation of those patches into a more continuous urban fabric. Understanding this process requires moving beyond qualitative description toward the systematic, repeatable quantification of urban form over time.

1.2 Urban fragmentation in rapidly growing cities

Urban fragmentation is commonly invoked as the default descriptor of land-cover change in fast-growing developing-country cities: as built-up land expands, it is assumed to do so through the scattering of numerous small, disconnected patches across the urban fringe, producing a landscape that is simultaneously larger in extent and more fragmented in structure. This assumption is not without empirical support; studies of Chinese, Ghanaian, and several Nigerian cities have documented periods in which patch counts and edge densities rose sharply alongside built-up extent but it is only part of a more complex picture (Anane, 2026). Landscape-ecology research on North American and Asian metropolitan regions shows that urban growth more typically proceeds through alternating phases of diffusion (Bereitschaft & Debbage 2014), in which new, spatially isolated patches appear at the urban fringe, and coalescence, in which those patches expand and merge with the existing urban fabric, producing oscillating rather than monotonic trends in patch number, size, and connectivity over time (Dietzel et al., 2005a, 2005b). Distinguishing genuine fragmentation from the more complex diffusion–coalescence dynamic is therefore an empirical, not a definitional, question, and it is precisely this question that the Owerri case is well placed to answer.

1.3 Landscape metrics for quantifying urban form

Landscape metrics, quantitative indices originally developed within landscape ecology to describe the composition and spatial configuration of categorical land-cover mosaics, provide the principal toolkit for operationalising urban morphological change (McGarigal & Marks, 1995; McGarigal et al., 2002). Implemented in the widely used FRAGSTATS software, these metrics are computed at three levels: the patch level (individual built-up fragments), the class level (the built-up class as a whole, relative to all other land-cover classes), and the landscape level (the entire LULC

mosaic). Composition metrics such as the percentage of landscape occupied by a class (PLAND) describe how much of the landscape a class occupies without reference to its spatial arrangement, whereas configuration metrics describe how that area is arranged in space.

Patch density (PD) and number of patches (NP) capture the degree of subdivision of a class into discrete fragments; the largest patch index (LPI) captures the dominance of the single largest contiguous patch; edge density (ED) and the landscape shape index (LSI) capture the geometric complexity of patch boundaries; the Euclidean mean nearest-neighbour distance (ENN_MN) captures the average isolation of patches from one another; and the aggregation index (AI), patch cohesion index (COHESION), contagion index (CONTAG), and landscape division index (DIVISION) jointly capture the degree to which the class (or landscape) is clumped into a small number of large, well-connected patches as opposed to being dispersed into many small, isolated ones (Li & Reynolds, 1993; Schumaker, 1996). No single metric captures the full morphological signal; because several indices are mathematically or empirically correlated with one another, careful metric selection and redundancy screening (rather than the indiscriminate reporting of every available index) is required to produce an interpretable and non-redundant account of landscape structure.

1.4 Statement of Research Problem and Research Gap

The land-use trajectory of rapidly growing Nigerian and West African secondary cities has been documented in a growing body of case studies. In Uyo, Akwa Ibom State, built-up land expanded from 23.44% to 44.80% of the study area between 1986 and 2024, with vegetation and forest cover declining correspondingly (Ituen, 2025). In Enugu, built-up area rose from 4.21% in 1986 to 62.45% in 2021, alongside rising Shannon diversity values interpreted as increasing sprawl (Ekere & Ajayi, 2026). Studies of Kumasi and Accra, Ghana, report that peri-urban expansion has been accompanied by increased fragmentation and aggregation of built-up patches simultaneously, core areas consolidating even as the periphery sprawls outward through leapfrogging (Abass et al., 2018). Comparable dynamics have been reported for Kampala and Mbarara in Uganda, where built-up land rose from 7.14% to 55.10% and from 6.37% to 30.95% respectively between the late 1980s/early 2000s and the mid-2010s, at the expense of agricultural land (Muchelo et al., 2024). Nigeria-focused planning research has repeatedly linked such unregulated expansion to fragmented governance, weak development control, and a widening mismatch between urban growth and infrastructure provision (Olaiya & Ajala, 2026; Nigeria Housing Market 2026).

Despite this substantial and growing literature, three gaps remain. First, most Nigerian LULC change studies stop at reporting the composition of land-cover classes over time (area and percentage change) without extending the analysis into the configuration domain of landscape ecology, that is, without asking not merely how much built-up land there now is, but how it is spatially organised. Second, where landscape metrics are used, they are typically reported for a single time slice or interpreted individually, rather than being read jointly, over multiple intervals, as evidence for or against a specific morphological process (such as diffusion–coalescence). Third, Owerri, the capital of Imo State and one of south-eastern Nigeria's principal secondary cities, features a rapidly expanding urban agglomeration population that grew from 501,000 residents in 2006 to over 1.1 million by 2026, driven by an

annual growth rate hovering around 4% according to UN World Urbanization Prospects data. This has been the subject of hazard-oriented geospatial studies (Ibeabuchi & Chibuike, 2024) but has not previously been the subject of a dedicated, multi-decadal, metric-based morphological transformation study spanning 1990–2025.

1.5 Aim and objectives

The aim of this study is to quantify and interpret the morphological transformation of the Owerri Urban Area between 1990 and 2025 using class- and landscape-level spatial metrics, in order to establish whether that transformation is better characterised as simple fragmentation or as a more complex, multi-stage morphological process. Four objectives operationalise this aim:

i. Quantify the temporal transformation of urban landscape structure in Owerri Urban Area from 1990 to 2025 using class-level and landscape-level spatial metrics.

ii. Evaluate changes in the size, shape, aggregation, connectivity, and fragmentation of built-up patches across the study period.

iii. Identify the dominant morphological patterns and phases of urban expansion through temporal analysis of patch configuration and spatial expansion forms.

iv. Characterize the temporal morphological transition of Owerri's urban form across distinct development stages.

2.0 Materials and Methods

2.1 Study area

Owerri Urban Area comprises the built-up core and immediately surrounding administrative territory of Owerri, the capital of Imo State in south-eastern Nigeria, situated within the humid tropical rainforest belt of the Niger Delta hinterland. Geographically situated near latitude 5.489°N and longitude 7.018°E, it encompasses Owerri Municipal, Owerri North, and Owerri West Local Government Areas and their immediate peri-urban fringe, has undergone a marked administrative and demographic transformation since Owerri was designated capital of the newly created Imo State in 1976 (Owerri history sources; Past Cities, 2026).

This designation catalysed sustained public investment in roads, tertiary institutions (including the Federal University of Technology Owerri, Imo State University, and Alvan Ikoku Federal College of Education), and administrative infrastructure, transforming what had been a modest trading and administrative town into a metropolitan agglomeration whose population is estimated to have grown from roughly half a million in the mid-2000s to over one million by the mid-2020s (UN, 2025). The area's physical geography, gently undulating lowland terrain, a dense network of streams and wetlands feeding the Otamiri and Nworie rivers, and predominantly ferralitic soils under a bimodal rainfall regime, has historically constrained development toward flatter, better-drained interfluves while leaving low-lying wetland corridors comparatively undeveloped.

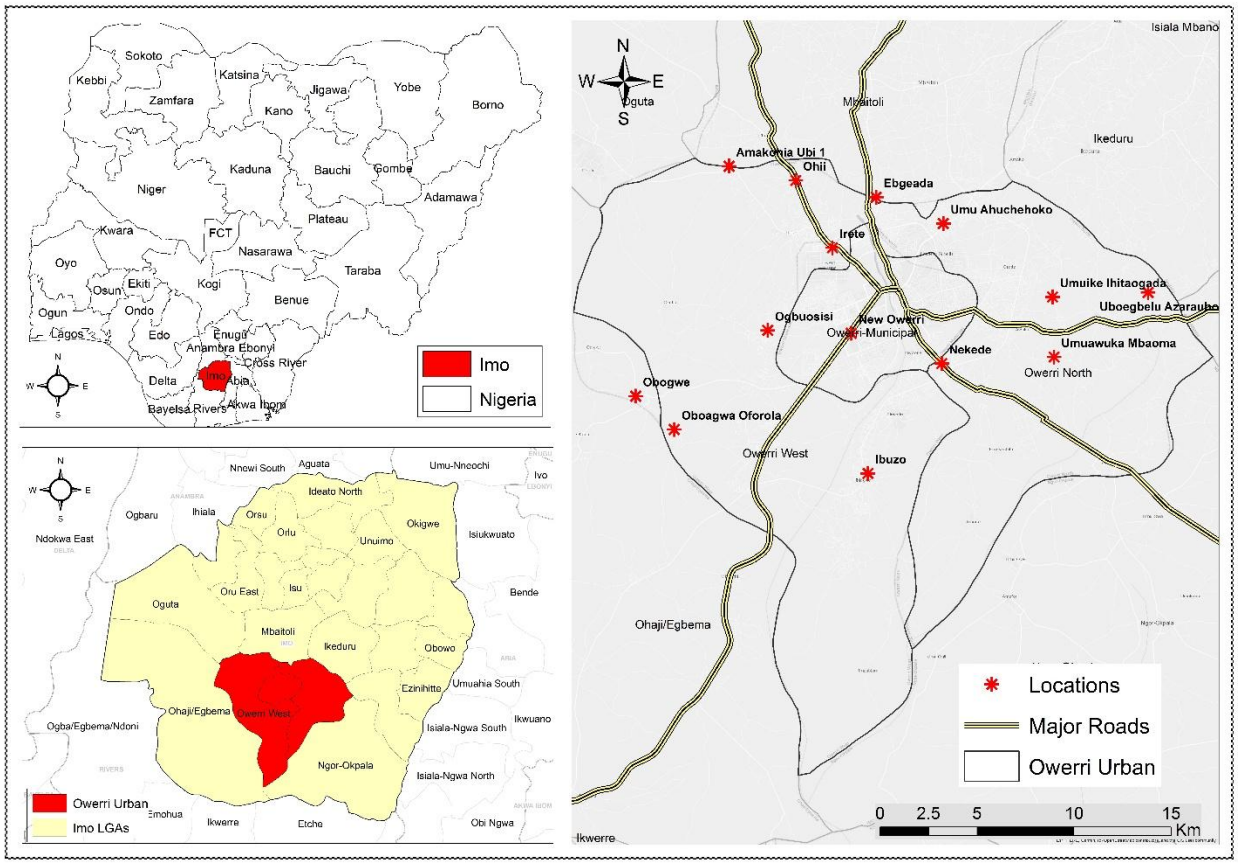


Fig 1: Map showing the Owerri Urban Area, Imo State

2.2 Methodology

2.2.1 Data Acquisition and Satellite Imagery Pre-processing

Multi-temporal satellite imagery covering the Owerri Urban Area was acquired from the United States Geological Survey (USGS) EarthExplorer platform for the years 1990, 2000, 2010, 2020, and 2025. All acquired scenes correspond to Path 188 / Row 055 and were selected during the dry season (December–February) to minimize atmospheric distortion and cloud cover (<5%). The imagery specifications and sensor metadata are summarized in Table 1.

Table 1. Landsat satellite imagery metadata used for LULC classification (1990–2025).

Target Year	Satellite / Sensor	Path / Row	Acquisition Date	Spatial Resolution (m)	Cloud Cover (%)
1990	Landsat 5 TM	188 / 055	1990-12-18	30	< 1.0%
2000	Landsat 7 ETM+	188 / 055	2000-01-12	30	< 2.0%
2010	Landsat 7 ETM+	188 / 055	2010-12-28	30	< 3.0%

2020	Landsat 8 OLI/TIRS	188 / 055	2020-01-08	30	< 1.0%
2025	Landsat 9 OLI-2/TIRS-2	188 / 055	2025-01-15	30	< 1.5%

2.2.2 Land Use / Land Cover (LULC) Classification Algorithm

Image classification was performed using the Random Forest (RF) machine learning algorithm in Google Earth Engine (GEE). Random Forest (RF) was selected over traditional Maximum Likelihood Classification (MLC) due to its non-parametric handling of high-dimensional spectral data, resilience to noise and training sample imbalances, and superior classification accuracy in complex urban-rural fringe environments. Training and validation sample points were extracted using stratified random sampling across six distinct LULC classes (Built-up, Bare Land, Agricultural Land, Vegetation, Wetland, and Water Body).

2.2.3 Spatial Pattern Analysis and FRAGSTATS Parameter Settings

To quantify the morphological transformation and spatial configuration of urban growth, class-level landscape metrics were computed for the Built-up class across all five target years. Landscape metrics were extracted using FRAGSTATS (Version 4.2). To ensure spatial consistency and reproducibility across all observation periods, the software execution settings were configured as follows:

- **Software Environment:** FRAGSTATS v4.2
- **Input Raster Grid Size:** 30m by 30m (Landsat Data)
- **Coordinate Reference System:** WGS 1984 / UTM Zone 32N (EPSG: 32632)
- **Neighborhood Connectivity Rule:** 8-neighbour (queen's case) connectivity rule for patch delineation
- **Target Class:** Built-up Class (Class ID 1)

2.3 Historical LULC datasets

Land use/land cover (LULC) information for five epochs — 1990, 2000, 2010, 2020, and 2025 — was derived from multi-temporal Landsat imagery (Thematic Mapper, Enhanced Thematic Mapper Plus, and Operational Land Imager sensors, as appropriate to each acquisition date), consistent with the standard multi-decadal LULC change-detection approach widely applied in Nigerian and West African urban studies (e.g., Ituen et al., 2025; Ekere & Ajayi, 2026). Each epoch was classified into six thematic classes (Table 2).

Table 2: Six-class land cover taxonomy for the Owerri Urban Area

LULC Class Code	Class Name	Operational Definition & Biophysical Description
1	Built-up Area	Impervious anthropogenic structures, including residential housing, commercial complexes, industrial facilities, paved transportation

		networks, tarmac, and concrete infrastructure.
2	Bare Land	Exposed soil surfaces, unpaved vacant plots, active construction clearings, excavated sites, fallow land stripped of cover, and eroded soil patches.
3	Agricultural Land	Cultivated croplands, subsistence agricultural fields, mixed farming areas, and sparse transitional crop vegetation.
4	Vegetation	Dense natural forest canopy, secondary forest regrowth, undisturbed bushland, riparian forest, and dense woody vegetation cover.
5	Wetlands	Low-lying, seasonally or permanently inundated marshy zones, saturated floodplains, and hydrophytic vegetation along river channels.
6	Water Body	Open surface water features, active tributaries, and retention ponds.

Accuracy Assessment

Classification performance for both RF and MLC across all historical baselines was evaluated using standard confusion matrices derived from the independent 20% validation sample. Performance was quantified using Producer's Accuracy (PA), User's Accuracy (UA), and Overall Accuracy (OA), the Kappa Coefficient (κ) (Table 3).

Table 3: Accuracy Assessment Metrics

Metric Name	Mathematical Expression	Analytical Description & Interpretation
Producer's Accuracy (PA)	$PA = \frac{Correctly\ Classifi}{Total\ reference\ pixels\ for}$	Probability that a ground truth reference pixel of class *i* is correctly classified on the map
User's Accuracy (UA)	$UA_i = \frac{n_{ii}}{n_{i+}} \times 100$	Probability that a pixel mapped as class *i* actually represents class *i* on the ground
Overall Accuracy (OA)	$OA_i = \frac{\sum_{i=1}^{r} n_{ii}}{N} \times 100$	Total proportion of correctly classified pixels across all categories relative to total reference sample N.
Kappa Coefficient (κ)	$\kappa = \frac{N\sum_{i=1}^{r} x_{ii} - \sum_{i=1}^{r} (x_{i+} \cdot x_{+i})}{N^2 - \sum_{i=1}^{r} (x_{i+} \cdot x_{+i})}$	Measure of classification agreement corrected for agreement expected purely by chance (κ > 0.75 indicates strong agreement).

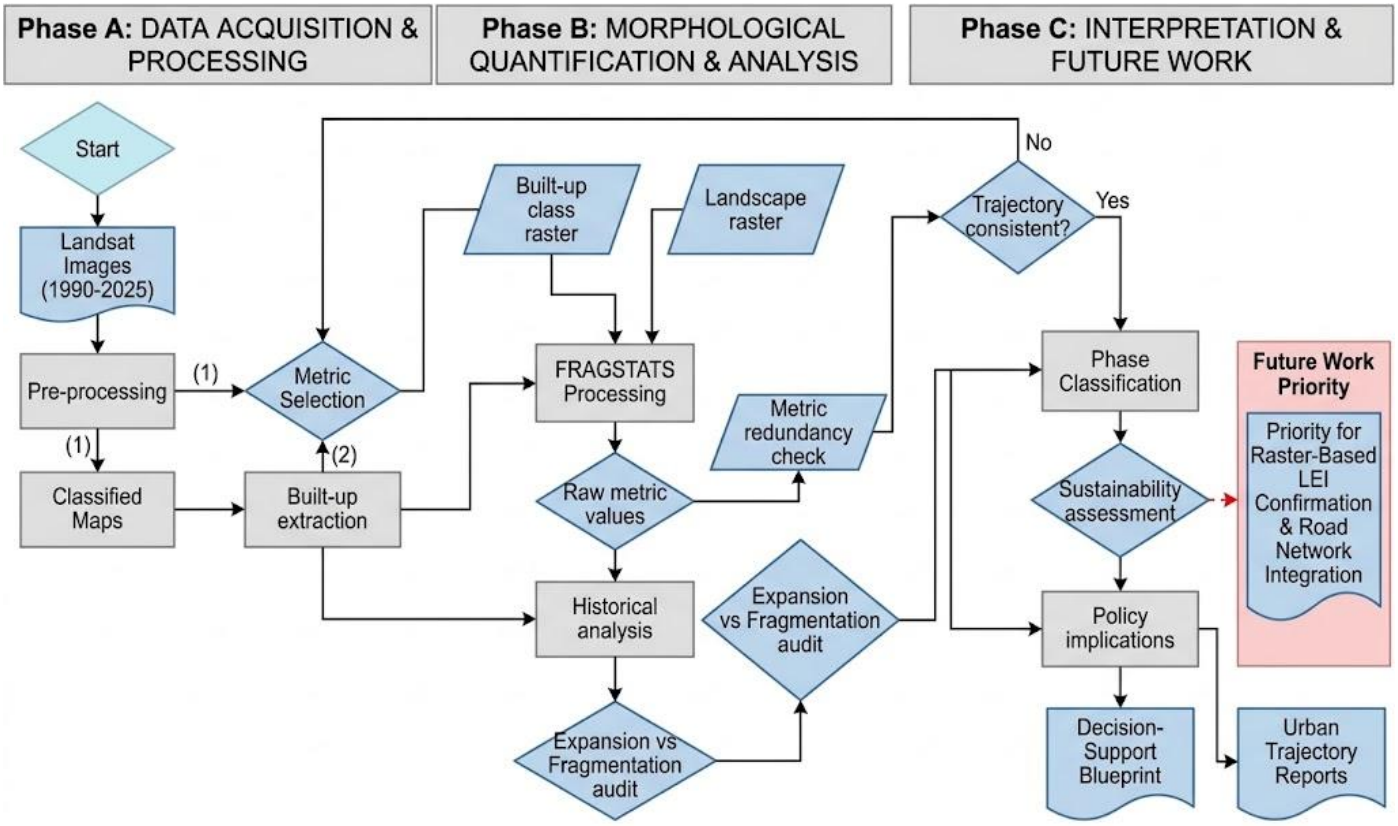


Figure 2: Methodology Workflow

Table 4: Random Forest Classification (1990) (Ground Truth vs Classified)

	Built ups	Bareland	Agric.	Veg.	Wetland	Waterbody	Total
Built-ups	7830	647	5	1	6	25	8514
Bareland	1288	6605	59	104	11	107	8174
Agric. Land	8	16	4251	245	0	3	4523
Vegetation	81	271	353	5594	22	39	6360
Wetland	11	18	2	16	257	12	316
Waterbody	6	16	1	2	4	338	367
Total	9224	7573	4671	5962	300	524	28254

Table 5: Random Forest Classification (2025) (Truth vs Classified)

	Built ups	Bareland	Agric.	Veg.	Wetland	Waterbody	Total

Built-ups	41985	12	0	32	0	237	42266
Bareland	21	8111	11	20	0	0	8163
Agric. Land	2	18	14745	88	0	3	14856
Vegetation	3	161	263	32503	2	0	32932
Wetland	0	0	0	0	257	0	257
Waterbody	1	0	0	0	0	4180	4181
Total	42012	8302	15019	32643	259	4420	102655

Table 6: Classification accuracy Random Forest (RF) for 1990 and 2025 baselines

Target Year	Classifier Model	Overall Accuracy (OA %)	Overall Kappa (κ)	Built-up User's Acc. (UA %)	Built-up Prod. Acc. (PA %)
1990	Random Forest (RF)	88.04%	0.8405	91.97%	84.89%
2025	Random Forest (RF)	99.15%	0.9878	99.34%	99.94%

2.4 Raster standardization

To ensure that the five classified maps were directly comparable and that patch- and class-level metrics computed from them were not artefacts of inconsistent processing, all rasters were standardised prior to metrics computation: reprojected to a common projected coordinate reference system, resampled to a common cell size, clipped to an identical 536.77 km² study-area boundary, and recoded to a common six-class legend with a consistent numeric class-coding scheme (cls_1 = built-up, cls_2 = bare land, cls_3 = agricultural land, cls_4 = vegetation, cls_5 = wetland, cls_6 = water body). This standardisation step is essential because FRAGSTATS metrics — particularly edge- and patch-based indices — are sensitive to cell size, projection distortion, and boundary effects, and inconsistent pre-processing across epochs would confound genuine temporal change with processing artefacts.

2.5 Built-up extraction

The built-up class (cls_1) was extracted from each of the five standardised classified rasters as a binary (built-up / non-built-up) layer for class-level FRAGSTATS analysis, while the full six-class raster was retained for landscape-level analysis. This dual approach allows the study to separately characterise (a) the internal morphology of the urban fabric itself — how built-up patches are structured, sized, and connected relative to one another — and (b) the structure of the wider LULC mosaic within which that urban fabric is embedded, an approach consistent with class-versus-landscape-level distinctions standard in landscape-ecology practice (McGarigal & Marks, 1995).

2.6 Landscape metrics

Landscape pattern metrics were computed for each of the five epochs using FRAGSTATS (McGarigal & Marks, 1995; McGarigal et al., 2002), applying the eight-neighbour (queen's case) cell-adjacency rule standard for urban/built-up patch delineation. At the class level, nine metrics were computed for the built-up class: percentage of landscape (PLAND), number of patches (NP), patch density (PD), largest patch index (LPI), edge density (ED), landscape shape index (LSI), Euclidean mean nearest-neighbour distance (ENN_MN), patch cohesion index (COHESION), and aggregation index (AI). At the landscape level, eight metrics were computed across the full six-class mosaic: patch density (PD), edge density (ED), landscape shape index (LSI), contagion index (CONTAG), percentage of like adjacencies (PLADJ), landscape division index (DIVISION), Shannon's diversity index (SHDI), and aggregation index (AI).

Table 7: Landscape Metrics definition (Turner, 1989)

Percentage of Landscape (PLAND): Measures the proportion of the total landscape occupied by the built-up class	$PLAND = P_i = \left(\frac{\sum_{j=1}^{n} a_{ij}}{A}\right) \times 100$
Number of Patches (NP): Total count of discrete built-up patches. Patch Density (PD): Number of built-up patches per 100 hectares	$PD = \frac{n_i}{A} \times 10{,}000 \times 100$
Largest Patch Index (LPI): Percentage of total landscape area comprised by the single largest built-up patch	$LPI = \left(\frac{max(a_{ij})}{A}\right) \times 100$
Edge Density (ED): Total length of built-up perimeter edge per unit landscape area (m/ha)	$ED = \frac{\sum_{k=1}^{m} e_{ik}}{A} \times 10{,}000$
Landscape Shape Index (LSI): Measures the shape complexity of built-up patches relative to a standard square	$LSI = \frac{0.25 \sum_{k=1}^{m} e_{ik}^{*}}{\sqrt{A}}$
Mean Euclidean Nearest-Neighbor Distance (ENN_MN): Mean shortest edge-to-edge distance between built-up patches	$ENN_{MN} = \frac{\sum_{j=1}^{n} h_{ij}}{n_i}$
Patch Cohesion Index (COHESION): Quantifies the physical connectedness of the built-up class. Aggregation Index (AI): Measures the frequency of like-adjacencies among built-up pixels (%).	$AI = \left(\frac{g_{ii}}{\max g_{ii}}\right) \times 100$

2.7 Morphological expansion analysis

Beyond the static, single-epoch interpretation of each metric, morphological expansion was assessed dynamically by computing, for the built-up class, the absolute change ($\Delta M = M_{2025} - M_{1990}$) and percentage change ($\%\Delta M = [(M_{2025} - M_{1990}) / M_{1990}] \times 100$) in each metric over the full study period, and by repeating this calculation separately for each of the four inter-census intervals (1990–2000, 2000–2010, 2010–2020, 2020–2025). Reading the direction and magnitude of change jointly across the patch-proliferation metrics (NP,

PD), the dominance metric (LPI), the aggregation/connectivity metrics (AI, COHESION, ENN_MN), and the edge/shape metrics (ED, LSI) within each interval allows specific morphological processes (proliferation, coalescence and consolidation, while identifying evidence of late-stage spatial restructuring where supported by the metrics) to be distinguished from one another, following the logic of the diffusion–coalescence framework (Dietzel et al., 2005a, 2005b) and of landscape-expansion-index-based urban growth typologies (infilling, edge-expansion, and outlying/leapfrog growth; Liu et al., 2010).

To assess redundancy among the nine built-up class-level metrics prior to their interpretive use, a descriptive Pearson correlation matrix was computed across the five epochs (n = 5 paired observations per metric pair). Given the small number of temporal observations, this matrix was used strictly as a tool for identifying which metrics carry substantially overlapping temporal signal and are therefore candidates for exclusion from the core narrative to avoid double-counting a single underlying process, rather than as a basis for inferential (significance-testing) claims, which would not be statistically defensible with only five time points.

3.0 Results

3.1 Changes in built-up landscape composition

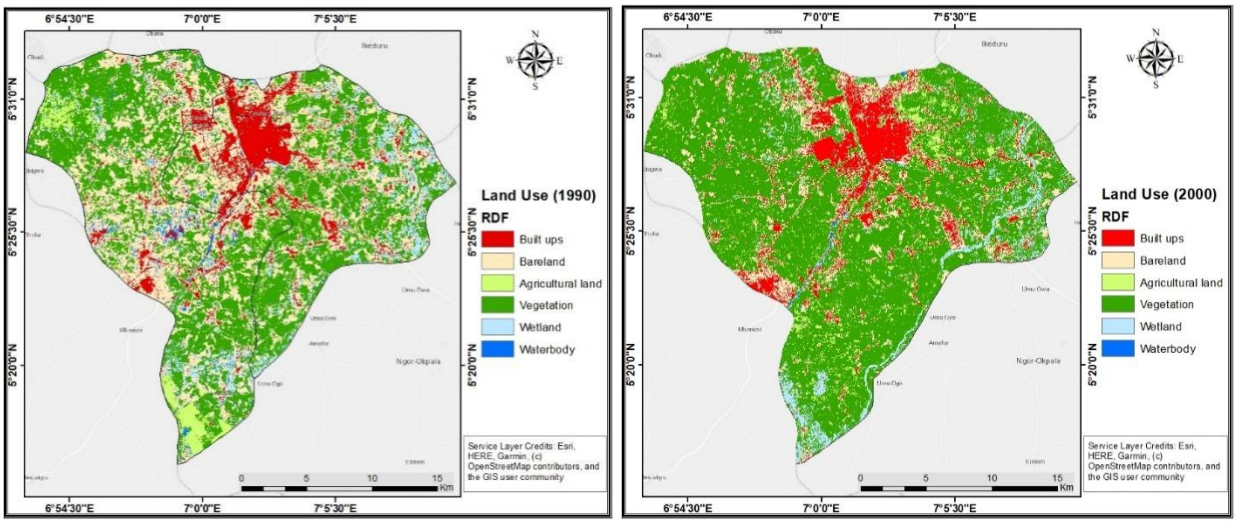
Table 8 presents the area and percentage composition of each LULC class across the five epochs. Built-up land increased almost continuously and substantially, from 50.42 km² (9.39%) in 1990 to 54.12 km² (10.08%) in 2000, 138.86 km² (25.87%) in 2010, 237.85 km² (44.31%) in 2020, and 244.80 km² (45.61%) in 2025. Vegetation, the dominant class in 1990 (42.08%), declined steadily to 26.14% by 2025. Bare land fell sharply between 1990 and 2000 (from 36.76% to 13.58%) and then stabilised around 12–14% for the remainder of the study period. Wetland collapsed from 4.40% in 1990 to a low of 0.26% in 2010, recovering only marginally to 0.29% by 2025, while water body declined from 3.55% to around 1.25–1.40% after an initial sharp drop by 2000. Agricultural land followed a more irregular path, rising from 3.82% (1990) to 6.14% (2010), falling back to 4.99% (2020), and then rising sharply to 12.81% by 2025.

Table 8. Area and percentage composition of each LULC class, Owerri Urban Area, 1990–2025.

LULC Class	1990 km² (%)	2000 km² (%)	2010 km² (%)	2020 km² (%)	2025 km² (%)
Built-up	50.42 (9.39)	54.12 (10.08)	138.86 (25.87)	237.85 (44.31)	244.80 (45.61)
Bare Land	197.31 (36.76)	72.91 (13.58)	64.94 (12.10)	67.33 (12.54)	74.65 (13.91)
Agricultural Land	20.49 (3.82)	20.74 (3.86)	32.98 (6.14)	26.80 (4.99)	68.75 (12.81)
Vegetation	225.89	358.64	296.35	194.74	140.33

LULC Class	1990 km² (%)	2000 km² (%)	2010 km² (%)	2020 km² (%)	2025 km² (%)
	(42.08)	(66.82)	(55.21)	(36.28)	(26.14)
Wetland	23.60 (4.40)	29.03 (5.41)	1.38 (0.26)	2.52 (0.47)	1.56 (0.29)
Water Body	19.06 (3.55)	1.32 (0.25)	2.26 (0.42)	7.52 (1.40)	6.68 (1.24)
Total Study Area	536.77 (100.0)	536.77 (100.0)	536.77 (100.0)	536.77 (100.0)	536.77 (100.0)

Table 9 summarises net change over the full 1990–2025 period. Built-up land recorded the largest absolute and percentage gain of any class (+194.38 km², +385.52%; compound annual rate of change, r = +4.61%), classified as continuous expansion. Agricultural land also expanded substantially (+48.26 km², +235.53%; r = +3.46%), a moderate expansion that, combined with the sharp 2020–2025 uptick evident in Table 7, may partly reflect renewed peri-urban farming activity on the urban fringe or reclassification associated with fallow/regrowth dynamics. All other classes declined: bare land recorded a substantial loss (−122.66 km², −62.17%; r = −2.78%), vegetation a systematic depletion (−85.56 km², −37.88%; r = −1.36%), water body a significant shrinkage (−12.38 km², −64.95%; r = −3.00%), and wetland the most severe proportional collapse of any class (−22.04 km², −93.39%; r = −7.76%).



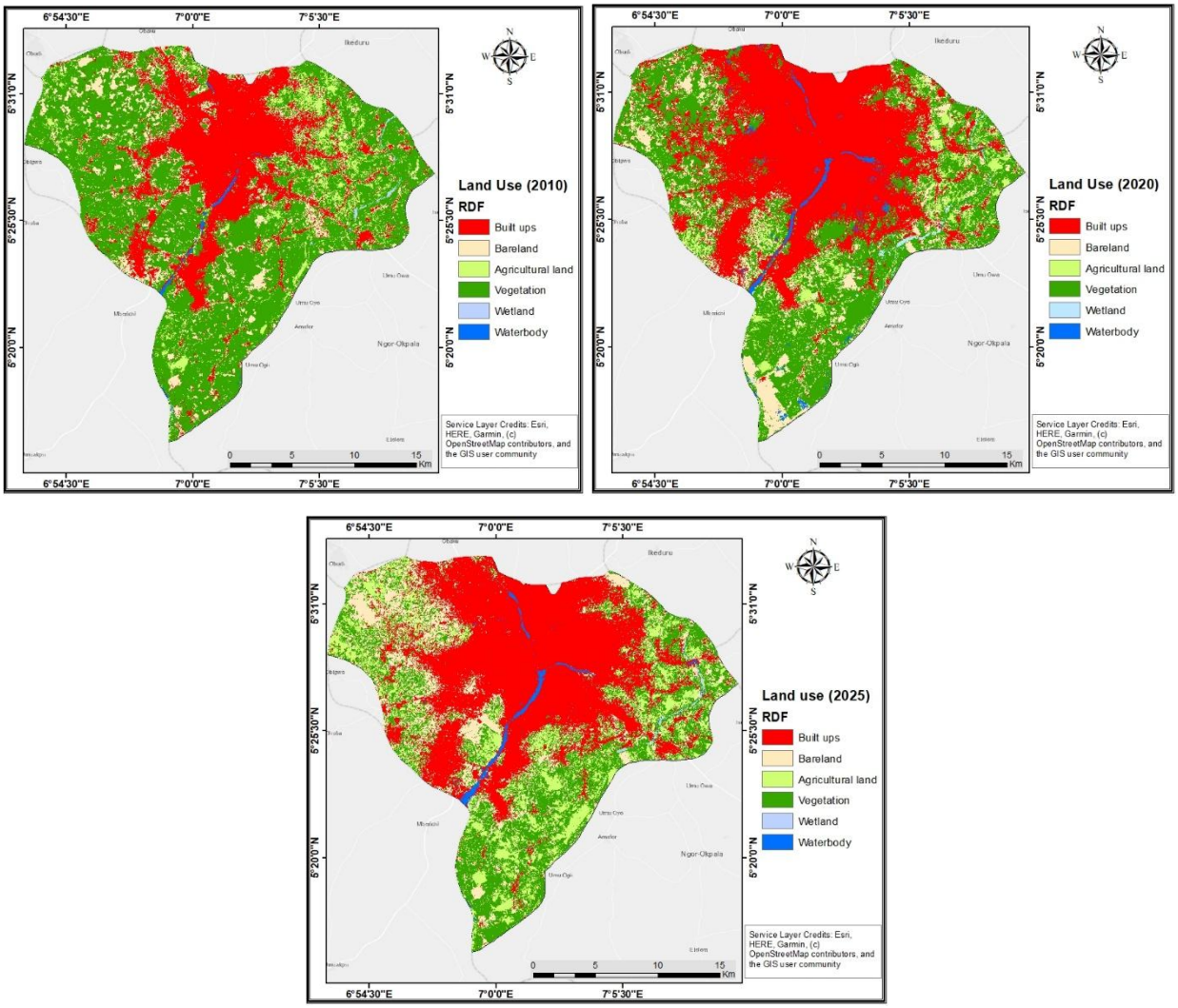


Figure 3: Land Use Land Cover Extent (1990 – 2025)

Table 9. Net change in LULC composition, 1990–2025 (CAGR = compound annual growth/change rate).

LULC Class	1990 (km²)	2025 (km²)	Net Change (km²)	% Change	CAGR (%)	Trajectory
Built-up	50.42	244.80	+194.38	+385.52	+4.61	Continuous Expansion
Bare Land	197.31	74.65	−122.66	−62.17	−2.78	Substantial Loss
Agric. Land	20.49	68.75	+48.26	+235.53	+3.46	Moderate Expansion

LULC Class	1990 (km²)	2025 (km²)	Net Change (km²)	% Change	CAGR (%)	Trajectory
Vegetation	225.89	140.33	−85.56	−37.88	−1.36	Systematic Depletion
Wetland	23.60	1.56	−22.04	−93.39	−7.76	Severe Collapse
Water Body	19.06	6.68	−12.38	−64.95	−3.00	Significant Shrinkage

The post-classification transition matrix (Table 10) confirms that the great majority of new built-up land in 2025 was converted from formerly non-built-up classes rather than from redevelopment of already-built land: of the 244.08 km² classified as built-up in 2025, only 46.38 km² (16.9%) had already been built-up in 1990, while 114.44 km² (41.8%) had been bare land, 85.84 km² (31.3%) had been vegetation, 9.22 km² (3.4%) had been agricultural land, 15.34 km² (5.6%) had been wetland, and 2.86 km² (1.0%) had been water body in 1990. Bare land was thus the single largest source of new built-up area, consistent with the widespread practice in rapidly urbanising Nigerian cities of clearing and levelling marginal or previously degraded land ahead of vegetation-covered land for construction, though vegetation conversion was also substantial in absolute terms.

Table 10. Post-classification transition matrix, 1990–2025 (km²).

1990 \ 2025	Built-up	Bare Land	Agric.	Vegetation	Wetland	Water	Total 1990
Built-up	46.38	2.02	1.01	0.51	0.00	0.50	50.42
Bare Land	102.16	35.51	23.68	32.01	1.97	1.98	197.31
Agric. Land	9.22	3.07	5.12	2.46	0.41	0.21	20.49
Vegetation	68.84	22.59	36.70	93.25	2.26	2.25	225.89
Wetland	15.34	2.83	1.89	2.36	0.94	0.24	23.60
Water Body	2.86	8.63	0.35	0.00	0.00	7.22	19.06
Total 2025	244.80	74.65	68.75	140.33	1.56	6.68	536.77

3.2 Built-up patch morphology

Table 11 presents the nine class-level FRAGSTATS metrics used to characterise the spatial morphology of the built-up class across the five observation years. The results indicate a substantial transformation in both the extent and spatial organisation of built-up land between 1990 and 2025.

PLAND increased from 9.3938% in 1990 to 45.6062% in 2025, representing an absolute increase of 36.2124 percentage points and a relative increase of 385.43%. This substantial increase confirms the expansion of built-up land as a major component of the landscape over the study period. The pattern is consistent with the land-use composition presented in Table 7.

The number of built-up patches (NP), however, exhibited a non-monotonic trajectory. NP increased from 2,381 patches in 1990 to 4,417 in 2000 and 4,929 in 2010, before declining to 3,455 in 2020 and 3,310 in 2025. This pattern suggests that urban expansion was initially accompanied by an increase in the number of discrete built-up patches, followed by a reduction in patch numbers as previously separated areas became increasingly connected or merged. Thus, the results do not support a simple interpretation of continuous fragmentation throughout the study period. Patch density (PD) followed the same trajectory, increasing from 4.4358 patches per 100 ha in 1990 to 9.1828 in 2010, before declining to 6.4367 in 2020 and 6.1665 in 2025, reflecting its direct relationship with NP.

The largest patch index (LPI) showed a markedly different pattern. LPI increased from 5.2037% in 1990 to 21.0788% in 2010 and 40.4516% in 2020, reaching 41.8200% in 2025. This substantial increase indicates that an increasingly large proportion of the built-up class became concentrated within the largest contiguous or dominant built-up patch. The simultaneous decline in NP and PD after 2010, together with the continued increase in LPI, suggests a shift from a landscape characterised by numerous smaller built-up patches towards a more spatially consolidated urban structure.

Edge density (ED) increased consistently from 27.0302 m/ha in 1990 to 57.8500 m/ha in 2025, indicating a substantial increase in the amount of built-up edge relative to the landscape area. Landscape Shape Index (LSI), by contrast, followed a more irregular trajectory. It increased sharply from 51.1667 in 1990 to 72.7149 in 2000, corresponding with the period of highest patch proliferation, before declining to 58.0496 in 2010, 49.5879 in 2020 and 48.2100 in 2025. The decline in LSI after 2000 suggests that the built-up landscape progressively became less characterised by complex or dispersed patch configurations as expansion increasingly occurred through the enlargement and joining of existing built-up areas.

The mean Euclidean nearest-neighbour distance (ENN_MN) also declined progressively, from 106.9208 m in 1990 to 83.1200 m in 2025, indicating increasing spatial proximity among built-up patches. This reduction, alongside the increase in LPI, provides further evidence of growing spatial integration within the built-up landscape. Similarly, the Aggregation Index (AI) increased from 78.6881 in 1990 to 91.1500 in 2025, indicating a substantial increase in the degree to which built-up cells became spatially aggregated. Patch cohesion remained consistently high, increasing from 98.3305 to 99.8210, suggesting that the built-up class maintained strong physical connectedness throughout the period, with further consolidation over time.

Overall, the metrics reveal a two-stage morphological transformation. The earlier period, particularly 1990–2010, was

characterised by rapid increases in patch number, patch density and landscape-shape complexity, consistent with the emergence and proliferation of separate built-up patches. From 2010 onwards, the decline in NP and PD, combined with increasing LPI, ENN_MN reduction, AI and cohesion, indicates a transition towards greater aggregation, connectivity and spatial consolidation. The morphology therefore reflects not simply increasing fragmentation, but an initial phase of patch proliferation followed by progressive coalescence and consolidation of the urban landscape.

.

Table 11. Class-level FRAGSTATS metrics for the built-up class (cls_1), 1990–2025.

Year	PLAND (%)	NP	PD	LPI (%)	ED	LSI	ENN_MN	COHESION	AI
1990	9.3938	2,381	4.4358	5.2037	27.0302	51.1667	106.9208	98.3305	78.6881
2000	10.0831	4,417	8.2289	4.8517	39.7425	72.7149	103.8685	97.7183	70.6030
2010	25.8703	4,929	9.1828	21.0788	50.7367	58.0496	92.3405	99.4778	85.4317
2020	44.3114	3,455	6.4367	40.4516	56.4984	49.5879	85.6400	99.7966	90.5223
2025	45.6062	3,310	6.1665	41.8200	57.8500	48.2100	83.1200	99.8210	91.1500

3.3 Landscape fragmentation and aggregation

Table 12 reports the eight landscape-level metrics computed across the full six-class LULC mosaic. Landscape PD followed a U-shaped trajectory, falling from 52.06 in 1990 to a low of 36.50 in 2010, then rising back to 51.64 by 2025, as did ED and LSI, both of which fell to their study-period minima in 2010 (119.36 and 70.60, respectively) before recovering toward their 1990 levels by 2025. The landscape division index (DIVISION), a measure of the probability that two randomly chosen points in the landscape lie in different patches, where lower values indicate a less subdivided landscape, fell from 0.9151 in 1990 to 0.8055 in 2000, rose again to 0.8844 in 2010, and then settled around 0.81–0.83 for 2020–2025; overall, DIVISION in 2025 (0.8271) remained below its 1990 value, indicating that the landscape as a whole was, on balance, less subdivided at the end of the study period than at its start, despite the built-up class occupying a far larger share of it. CONTAG and AI at the landscape level both peaked around 2000–2010 (CONTAG: 51.88 in 2000; AI: 82.10 in 2010) before easing back toward, but not below, their 1990 levels by 2025, while PLADJ followed a similar peak-in-the-middle pattern.

Table 12. Landscape-level FRAGSTATS metrics for the full six-class LULC mosaic, 1990–2025.

Year	PD	ED	LSI	CONTAG	PLADJ	DIVISION	SHDI	AI
1990	52.0563	161.6041	95.0592	41.0940	75.5671	0.9151	1.3348	75.7655
2000	43.6243	141.3316	83.3207	51.8757	78.6079	0.8055	1.0702	78.7885
2010	36.5001	119.3577	70.5971	51.4053	81.9040	0.8844	1.1430	82.1011
2020	40.1162	124.4790	73.5625	48.1365	81.1358	0.8094	1.2235	81.3369
2025	51.6352	151.2471	89.0621	42.5063	77.1206	0.8271	1.3395	77.3216

3.4 Spatial connectivity/cohesion

The connectivity and isolation metrics indicate continued spatial integration of the built-up class through 2025. COHESION increased from 98.33 in 1990 to 99.82 in 2025, while AI increased from 78.69 to 91.15. ENN_MN declined from 106.92 m in 1990 to 83.12 m in 2025, indicating that built-up patches became progressively closer to one another. Between 2020 and 2025, ENN_MN declined further from 85.64 m to 83.12 m, while AI increased from 90.52 to 91.15 and COHESION remained essentially unchanged at approximately 99.8. Taken together, these metrics indicate that the high level of spatial consolidation achieved by 2020 was maintained and strengthened slightly through 2025 rather than being followed by a clear reversal.

3.5 Morphological expansion patterns

Table 13 presents the percentage change in each retained built-up metric across the four inter-epoch intervals, forming the empirical basis for the phase classification. The 1990–2000 interval combines only modest PLAND growth (+7.34%) with sharp increases in NP (+85.51%), PD (+85.51%), ED (+47.03%), and LSI (+42.11%), alongside a fall in AI (−10.27%) and a slight fall in COHESION (−0.62%), the configurational signature of numerous new, relatively small, dispersed built-up patches appearing across the study area, consistent with a diffusion-dominated growth mode (Dietzel et al., 2005a, 2005b). The 2000–2010 interval shows a sharp acceleration in PLAND (+156.57%) combined with only a modest further rise in NP (+11.59%) but a very large rise in LPI (+334.46%) and a substantial rise in AI (+21.00%) alongside falling ENN_MN (−11.10%), indicating that expansion during this decade occurred predominantly through the growth and merging of existing patches (coalescence) rather than through further proliferation of new, isolated ones.

The 2010–2020 interval shows the clearest coalescence signature of the whole study period: NP and PD both fell by 29.90% even as LPI rose by a further 91.91% and AI and COHESION continued to rise, a pattern only explicable by the merging of previously separate built-up patches into fewer, much larger, more contiguous units (Liu et al., 2010). Finally, the 2020–2025 interval shows a modest continuation of the

consolidated pattern. NP and PD declined by 4.20%, while LPI increased by 3.38%, ENN_MN declined by 2.94%, and AI increased slightly by 0.69%. Together, these changes indicate that the highly consolidated built-up structure established by 2020 was maintained and strengthened marginally through 2025, rather than undergoing a clear return to dispersed patch formation.

Table 13. Percentage change in built-up class metrics across the four inter-epoch intervals.

Metric	1990–00	2000–10	2010–20	2020–25
PLAND	+7.34%	+156.57%	+71.28%	+2.92%
NP / PD	+85.51%	+11.59%	−29.90%	−4.20%
LPI	−6.76%	+334.46%	+91.91%	+3.38%
ED	+47.03%	+27.66%	+11.36%	+2.39%
LSI	+42.11%	−20.17%	−14.58%	−2.78%
ENN_MN	−2.85%	−11.10%	−7.26%	−2.94%
COHESION	−0.62%	+1.80%	+0.32%	+0.02%
AI	−10.27%	+21.00%	+5.96%	+0.69%

Metric redundancy (descriptive correlation analysis)

The descriptive Pearson correlation matrix among the nine built-up metrics (n = 5 epochs; Table 134) confirms substantial redundancy among several metric pairs, consistent with their shared derivation or shared underlying process. PLAND and LPI are correlated at 1.000, reflecting that, over this study period, the growth of overall built-up extent and the growth of the single largest built-up patch tracked each other almost perfectly. COHESION and AI are correlated at 0.987, indicating that these two aggregation-type indices carry very similar temporal signal. NP and PD are, by mathematical construction, correlated at 1.000. PLAND is strongly negatively correlated with ENN_MN (−0.954) and strongly positively correlated with ED (0.914) and COHESION (0.924).

Table 14. Descriptive Pearson correlation matrix among nine built-up class metrics (n = 5 epochs).

	PLAND	NP	PD	LPI	ED	LSI	ENN	COHES.	AI

	PLAND	NP	PD	LPI	ED	LSI	ENN	COHES.	AI
PLAND	1.000	.158	.158	1.000	.914	-.605	-.954	.924	.920
NP	.158	1.000	1.000	.135	.538	.541	-.343	.155	.000
PD	.158	1.000	1.000	.135	.538	.541	-.343	.155	.000
LPI	1.000	.135	.135	1.000	.904	-.623	-.949	.925	.925
ED	.914	.538	.538	.904	1.000	-.266	-.955	.828	.761
LSI	-.605	.541	.541	-.623	-.266	1.000	.480	-.727	-.819
ENN_MN	-.954	-.343	-.343	-.949	-.955	.480	1.000	-.924	-.882
COHESION	.924	.155	.155	.925	.828	-.727	-.924	1.000	.987
AI	.920	.000	.000	.925	.761	-.819	-.882	.987	1.000

3.6 Temporal phases of urban morphological transformation

Four discrete morphological phases are identified for Owerri's built-up class over 1990–2025 (Table 15), directly addressing Objectives 3 and 4.

Table 15. The four-phase morphological trajectory of Owerri's built-up class, 1990–2025.

Period	Phase	Key evidence
1990–2000	Patch proliferation / dispersed expansion	NP +85.5%, PD +85.5%, LSI +42.1%, AI −10.3%, LPI −6.8%
2000–2010	Rapid expansion and coalescence	PLAND +156.6%, LPI +334.5%, AI +21.0%, ENN_MN −11.1%
2010–2020	Consolidation / urban coalescence	NP −29.9%, PD −29.9%, LPI +91.9%, AI +6.0%, COHESION +0.3%
2020–2025	Continued consolidation / stabilisation	NP −4.2%, PD −4.2%, LPI +3.4%, ENN_MN −2.9%, AI +0.7%

This sequence (proliferation, followed by coalescence, followed by consolidation, followed by renewed peripheral patch formation) is markedly different from, and more informative than, a simple summary statement that the number of built-up patches increased by 39.0% over the full study period would suggest, since such a summary would obscure the fact that the largest patch, aggregation, and cohesion metrics all rose even more sharply over the same period. The full-period change table (Table 16) is presented for reference and comparison with other published studies.

Table 16. Full-period (1990–2025) change in built-up class metrics, for reference.

Metric	1990	2025	Absolute Δ	% Δ
PLAND (%)	9.3938	45.6062	+36.2124	+385.49%
NP	2,381	3,310	+929	+39.02%
PD	4.4358	6.1665	+1.7307	+39.02%
LPI (%)	5.2037	41.8200	+36.6163	+703.66%
ED	27.0302	57.8500	+30.8198	+114.02%
LSI	51.1667	48.2100	−2.9567	−5.78%
ENN_MN	106.9208	83.1200	−23.8008	−22.26%
COHESION	98.3305	99.8210	+1.4905	+1.52%
AI	78.6881	91.1500	+12.4619	+15.84%

4.0 Discussion

4.1 Transformation of Owerri's urban form

The results show that Owerri experienced substantial urban expansion between 1990 and 2025. During this period, the built-up area increased considerably, becoming the dominant land-cover class by 2020 and replacing vegetation as the major component of the landscape. However, the expansion did not occur at the same rate or in the same spatial pattern throughout the study period. Instead, the city experienced changes in the distribution and arrangement of built-up areas, with periods of new development occurring alongside periods of expansion and merging of existing built-up patches.

The results suggest four broad stages of urban development: initial dispersed growth (1990–2000), coalescence (2000–2010), consolidation (2010–2020), and renewed peripheral development (2020–2025). These stages describe changes in the spatial structure of the city rather than distinct development processes that can be attributed to a single cause. The increase in built-up patches during 1990–2000 indicates that new development occurred in several separate locations. Between 2000 and 2020, the reduction in patch numbers and increase

in the dominance of the largest built-up patch suggest that previously separate developed areas became more connected or merged. From 2020 to 2025, the increase in patch numbers and average patch isolation suggests a return to more spatially separated development.

This pattern is consistent with the diffusion–coalescence model of urban growth proposed by Dietzel et al. (2005a, 2005b), which explains urban expansion as a process involving the formation of new built-up patches followed by the expansion and merging of existing patches. It also aligns with the Conzenian perspective that urban form develops through successive changes over time (Conzen, 1960 (cited in Whitehand et al., 2009), 2012). However, the landscape metrics alone cannot establish the precise historical or socioeconomic causes of each growth phase. The proposed stages should therefore be understood as interpretations of the observed spatial patterns, rather than direct evidence of specific development policies, infrastructure investments, or planning decisions.

4.2 Expansion versus fragmentation

The results indicate that Owerri's urban expansion between 1990 and 2025 involved both the formation of new built-up patches and the increasing dominance and connectivity of existing built-up areas. Therefore, the increase in the number of built-up patches should not automatically be interpreted as evidence of continuous or increasing fragmentation. Across the study period, the number of built-up patches increased by 39.0%. However, LPI increased much more substantially, by 703.7%, while AI increased by 15.8%. COHESION also increased by 1.5 percentage points from its already high 1990 value of 98.33 to 99.82. Taken together, these changes indicate that although the number of built-up patches increased over the full study period, the dominant morphological trend was toward greater aggregation, patch dominance, and spatial connectivity rather than continuous fragmentation.

The apparent difference between the increase in patch numbers and the improvement in connectivity can be explained by examining urban growth across different periods. Between 1990 and 2000, the number of built-up patches increased substantially, while the growth in built-up area remained relatively limited. This suggests that new development was distributed across multiple locations. In contrast, the period from 2000 to 2020 was characterised by a reduction in patch numbers and an increase in the size of the dominant built-up area, indicating greater consolidation. These findings support the use of a multi-metric approach to understanding urban expansion (Dietzel et al. 2005a, 2005b). A single increase in patch number does not necessarily demonstrate that the entire urban landscape has become more fragmented. Similarly, an increase in aggregation does not mean that all forms of peripheral development have ceased. Different growth processes can occur simultaneously in different parts of the city (Ekere & Ajayi, 2026). The results therefore demonstrate the importance of examining patch number, patch dominance, aggregation, and connectivity together when assessing urban morphological change. This approach provides a more comprehensive understanding of Owerri's expansion than relying on a single landscape metric.

4.3 Consolidation, edge growth and peripheral restructuring

The period between 2010 and 2020 represents the clearest phase of built-up consolidation in the study. During this period, the number of built-up patches decreased by 29.9%, while the Largest Patch

Index increased by 91.9%. This combination indicates that the built-up landscape became more concentrated within a dominant urban patch. The observed pattern is consistent with the expansion and merging of previously separate built-up areas. It may reflect the outward growth of established urban areas, the development of spaces between existing settlements, or a combination of both. However, the available landscape metrics cannot independently confirm whether this consolidation occurred primarily through edge expansion, infilling, or other forms of development.

The consolidation observed between 2010 and 2020 is broadly comparable to findings from studies of urban expansion in other African cities, including Kumasi, Accra, and Uyo, where researchers have identified the importance of outward urban growth and the expansion of established urban areas (Abbas et al., 2018; Ituen et al., 2025). The period from 2020 to 2025 presents a different but not contradictory pattern. Rather than showing renewed patch proliferation, NP and PD declined by 4.2%, while LPI increased by 3.4% and ENN_MN declined by 2.9%. AI also increased slightly, from 90.52 to 91.15. These changes indicate that the highly consolidated structure established by 2020 was maintained and became marginally more aggregated through 2025. The final interval therefore appears to represent a phase of continued consolidation or morphological stabilisation rather than a clear return to dispersed peripheral development.

These changes suggest that new built-up areas emerged outside the dominant urban patch or that some existing peripheral patches became more spatially separated. This pattern may be associated with peripheral expansion, leapfrog development, or the establishment of new residential and institutional areas. Nevertheless, the specific land-use activities responsible for these changes cannot be determined from the landscape metrics alone. The results highlight a shift from the stronger consolidation observed during 2010–2020 to a more dispersed pattern of built-up development during 2020–2025. This change deserves attention because continued peripheral expansion may create additional challenges for infrastructure provision, road connectivity, and coordinated land-use planning.

4.4 Implications for urban morphology and land management

The observed changes in Owerri's urban structure have important implications for urban planning, infrastructure provision, and land management. The period from 1990 to 2000 was characterised by a substantial increase in the number of built-up patches, which rose by 85.5%, while the total built-up area increased by only 7.3%. This suggests that new development occurred across multiple locations without a corresponding increase in the size of existing built-up areas. Such a pattern is consistent with dispersed urban expansion. Dispersed development can create difficulties for infrastructure provision, particularly where residential areas emerge faster than roads, drainage systems, water supply, and other essential services. However, the landscape metrics cannot establish whether these services were absent or inadequate in the newly developed areas. Field observations and infrastructure data would be required to confirm the relationship between spatial expansion and service provision.

Between 2000 and 2020, the reduction in patch numbers and increase in the dominance of the largest built-up patch indicate greater spatial consolidation. A more connected urban structure may create opportunities for more efficient

infrastructure provision. However, the actual benefits depend on the availability, quality, and distribution of infrastructure across the expanding urban area (Olaiya & Ajala., 2026; Ogunleye, 2015). The continued decline in patch numbers between 2020 and 2025, together with the modest increase in LPI and AI and further reduction in ENN_MN, suggests that the consolidated urban structure was maintained during the final interval. This does not imply that peripheral development ceased, but the available metrics do not provide sufficient evidence to characterise 2020–2025 as a renewed phase of dispersed patch formation. This finding provides an opportunity for planning authorities to monitor areas experiencing new development and assess whether infrastructure provision and land-use planning are keeping pace with expansion.

The conversion of natural land cover also requires attention. The study recorded a 93.4% decline in wetland cover by 2025, while the transition analysis showed that new built-up areas were derived from previously undeveloped land, including bare land and vegetation. These changes may have implications for surface runoff, drainage, and flood vulnerability, particularly where development occurs in environmentally sensitive areas. However, the relationship between land-cover conversion and flood risk requires additional analysis using drainage characteristics, elevation, rainfall, and flood-susceptibility data. The findings therefore support the need to integrate land-use monitoring with environmental risk assessment and infrastructure planning in Owerri (Ibeabuchi & Chibuike, 2024).

4.5 Comparison with other African secondary cities

Owerri's urban expansion shares similarities with patterns reported in other African cities, although the scale and spatial characteristics of growth differ across locations. The proportion of land classified as built-up in Owerri increased from 9.4% in 1990 to 45.6% in 2025. This expansion can be compared with reported changes in Uyo, where the built-up share increased from 23.4% to 44.8% between 1986 and 2024, and Enugu, where it increased from 4.2% to 62.5% between 1986 and 2021 (Ituen et al., 2025; Ekere & Ajayi, 2026). Similar changes have also been reported in selected Ugandan cities, including Kampala and Mbarara (Muchelo et al., 2024). These comparisons should be interpreted carefully because the studies may differ in their study periods, classification methods, spatial boundaries, and definitions of built-up land. Consequently, differences in reported percentages do not necessarily indicate differences in the underlying urban development processes.

A key contribution of the Owerri study is its examination of both the amount of built-up land and its spatial arrangement. While built-up area provides information about the extent of urban expansion, landscape metrics help explain how development is distributed across the landscape. The results show that Owerri experienced different patterns of urban expansion during the study period. The increase in patch numbers during 1990–2000 occurred alongside a period of limited built-up expansion, whereas the subsequent decline in patch numbers from 2010 onward coincided with increasing consolidation and aggregation. This demonstrates that urban expansion does not necessarily follow a single pattern throughout a city's development.

Similar combinations of consolidation and peripheral expansion have been reported in studies of Greater Kumasi and Accra (Abbas et al., 2018). Research on secondary cities in Ghana and Tanzania has also identified

different combinations of infilling, edge expansion, and corridor development (Sumari & Cobbina, 2026). These comparisons suggest that urban growth patterns vary according to local conditions, including land availability, infrastructure, settlement structure, and planning arrangements. Owerri's case contributes to the broader understanding of urban expansion in African secondary cities by demonstrating how landscape metrics can be used to examine changes in both the extent and spatial configuration of built-up land (Sondou et al., 2024). The findings also highlight the importance of studying secondary cities independently, rather than assuming that their development follows the same patterns as larger metropolitan areas (Korah et al., 2025; Anane, 2026).

5.0 Conclusion and Recommendations

5.1 Conclusion

This study quantified and characterised the morphological transformation of the Owerri Urban Area, Nigeria, across five temporal epochs from 1990 to 2025 using satellite remote sensing and class-level landscape metrics. Over the 35-year observation period, built-up land expanded nearly five-fold. This physical growth occurred primarily through the conversion of bare land and vegetation, alongside a severe reduction in wetland cover. Transition matrix modeling confirmed that bare land and vegetation served as the primary immediate source classes for built-up conversion. Spatial metric analysis (PLAND, NP, LPI, LSI, AI) revealed that urban expansion did not proceed as continuous fragmentation. Instead, built-up morphology evolved non-linearly. In general, the structural trajectory of Owerri transitioned through four distinct morphological phases: patch proliferation and dispersed expansion (1990–2000), rapid expansion and coalescence (2000–2010), consolidation (2010–2020), and continued consolidation with morphological stabilisation (2020–2025). This sequence provides empirical support for the diffusion–coalescence model of urban growth within secondary African cities.

5.2 Policy and Planning Recommendations

Based on the observed spatial patterns and landscape transformations, the following proactive planning strategies are proposed:

1. Proactive Peri-Urban Spatial Guidance: Planning authorities in Imo State should consider establishing targeted development guidelines along the urban fringe. The renewed patch-proliferation observed in the 2020–2025 phase highlights potential fringe sprawl, suggesting that proactive zoning could assist in maintaining contiguous urban growth.
2. Infrastructure Corridor Alignment: Aligning future road, utility, and drainage planning with identified spatial growth corridors may reduce future retrofitting costs and promote more orderly peripheral development.
3. Riparian Buffer Protection: In light of substantial wetland area reductions along the Otamiri and Nworie river catchments, environmental management authorities should consider establishing formal ecological protection zones in low-lying riparian areas to support localized flood mitigation.

5.3 Limitations and Future Research

While this study provides a multi-decadal evaluation of urban spatial structure in Owerri, several methodological and

analytical limitations highlight key directions for future research:

i. Aggregate Spatial Metrics: The reliance on class-level FRAGSTATS metrics quantifies overall landscape composition and structural configuration, but it does not differentiate pixel-level spatial growth modes (such as infill, edge-expansion, and leapfrog development). Future research should integrate a Landscape Expansion Index (LEI) to explicitly map local spatial growth typologies.

ii. Explanatory Spatial Drivers: This assessment focuses on satellite-derived land cover transitions without directly modeling underlying physical or socio-economic drivers. Incorporating multi-criteria spatial drivers, specifically road-network proximity and connectivity, infrastructure accessibility analysis (e.g., proximity to commercial nodes, power, and water distribution networks), and ground-level field validation, would enhance the explanatory capacity of future urban growth models.

iii. Hydrological and Risk Modeling: Rapid urban conversion of natural surfaces alters localized drainage behavior. Coupling future spatial growth projections with a detailed flood-risk assessment will be essential for identifying environmentally sensitive zones and supporting resilient urban spatial planning in Owerri

References

Abass, K., Adanu, S. K., & Agyemang, S. (2018). Peri-urbanisation and loss of arable land in Kumasi Metropolis in three decades: Evidence from remote sensing image analysis. *Land use policy*, *72*, 470-479. https://www.sciencedirect.com/science/article/abs/pii/S0264837717301746

Alrashdi, H., Shen, G., Chebika, H., & Mabrouk, M. (2026). Quantifying Urban Fragmentation through Urban Form: A Systematic Review and Integrative Assessment Framework. Sustainable Cities and Society, 107698. https://www.sciencedirect.com/science/article/abs/pii/S2210670726005810

Anane, G. K. (2026). 'Secondaryfication'and land use transitions: Spatio-temporal dynamics and growth trajectories in Ghana's emerging secondary cities. *Habitat International*, *173*, 103849.https://www.sciencedirect.com/science/article/abs/pii/S0197397526001426

Bereitschaft, B., & Debbage, K. (2014). Regional variations in urban fragmentation among US metropolitan and megapolitan areas. *Applied Spatial Analysis and Policy*, *7*(2), 119-147. https://link.springer.com/article/10.1007/s12061-013-9092-9

Dietzel, C., Herold, M., Hemphill, J. J., & Clarke, K. C. (2005a). Spatio-temporal dynamics in California's Central Valley: Empirical links to urban theory. International Journal of Geographical Information Science, 19(2), 175–195.

Dietzel, C., Oguz, H., Hemphill, J. J., Clarke, K. C., & Gazulis, N. (2005b). Diffusion and coalescence of the Houston metropolitan area: Evidence supporting a new urban theory. Environment and Planning B: Planning and Design, 32(2), 231–246.

Ekere, A. N., & Ajayi, D. D. (2026). Spatio-temporal dynamics of urban sprawl in Enugu metropolis, Nigeria (1986–2021): A GIS-based analysis. International Journal of Research and Innovation in Social Science, 10(6). https://doi.org/10.47772/IJRISS.2026.100600215

Ituen, U., Elijah, U. D., Jimmy, U. J., Udofia, U., Antai, B. E., Inwang, S., ... & Unyime, J. (2025). Spatial-temporal Dynamics of Urban Expansion and Land Cover Transformation in Uyo Capital City, Akwa Ibom State, Nigeria. Canadian Social Science, 21(4), 42-52. http://flr-journal.org/index.php/css/article/view/13837

Korah, A., Smith, L. C., & Wimberly, M. C. (2025). Understanding urban expansion across primary and secondary cities in Ghana. *Habitat International*, *158*, 103339. ScienceDirect. https://www.sciencedirect.com/science/article/pii/S0197397525000554

Li, H., & Reynolds, J. F. (1993). A new contagion index to quantify spatial patterns of landscapes. Landscape Ecology, 8(3), 155–162.

Liu, X., Li, X., Chen, Y., Tan, X., Liu, S., & Ai, B. (2010). A new landscape index for quantifying urban expansion using multi-temporal remotely sensed data. Landscape Ecology, 25, 671–682. https://doi.org/10.1007/s10980-010-9454-5

McGarigal, K., & Marks, B. J. (1995). FRAGSTATS: Spatial pattern analysis program for quantifying landscape structure (General Technical Report PNW-GTR-351). USDA Forest Service, Pacific Northwest Research Station.

McGarigal, K., Cushman, S. A., Neel, M. C., & Ene, E. (2002). FRAGSTATS: Spatial pattern analysis program for categorical maps. University of Massachusetts, Amherst.

Muchelo, R. O., Bishop, T. F., Ugbaje, S. U., & Akpa, S. I. (2024). Patterns of urban sprawl and agricultural land loss in sub-Saharan Africa: the cases of the Ugandan cities of Kampala and Mbarara. *Land*, *13*(7), 1056. https://doi.org/10.3390/land13071056

Nigeria Housing Market. (2026). Experts warn of deepening urban planning crisis in Nigeria. https://www.nigeriahousingmarket.com/news/nigeria-urban-planning-crisis-warning

Noaime, E., & Alnaim, M. M. (2025). Toward an Integrative Framework of Urban Morphology: Bridging Typomorphological, Sociological, and Morphogenetic Traditions. *Land*, *14*(12), 2323. https://doi.org/10.3390/land14122323

Ogunleye, O. (2015). One city, different realities: Infrastructure development and urban fragmentation in Nigeria. UCL Bartlett Development Planning Unit Blog. https://blogs.ucl.ac.uk/dpublog/2015/07/22/one-city-different-realities-infrastructure-development-urban-fragmentation-nigeria/

Olaiya, R. O., & Ajala, O. A. (2026). Integrating geo-spatial analysis and micro-level land use typologies for sustainable urban planning in Nigeria. *Discover Cities*, *3*(1), 111. https://link.springer.com/article/10.1007/s44327-026-00299-9

Past Cities. (2026). Past cities — Owerri, Imo, Nigeria. https://www.pastcities.com/showitem.php?item=owerri-imo-nigeria

Pratomoatmojo, N. A., Koomen, E., & de Groot, H. L. (2026). Uncovering merging and joining as urban expansion processes. *Computers, Environment and Urban Systems*, *127*, 102423. https://www.sciencedirect.com/science/article/pii/S0198971526000256

Schumaker, N. H. (1996). Using landscape indices to predict habitat connectivity. Ecology, 77(4), 1210–1225.

Sondou, T., Anoumou, K. R., Aholou, C. C., Chenal, J., & Pessoa Colombo, V. (2024). Urban growth and land artificialization in secondary African cities: A spatiotemporal analysis of Ho (Ghana) and Kpalimé (Togo). *Urban Science*, *8*(4), 207. https://www.mdpi.com/2413-8851/8/4/207

Sumari, N. S., & Cobbinah, P. B. (2026). Secondary cities in African urbanization: On urban expansion and density patterns in Tanzania's mid-sized cities. *Applied Geography*, *186*, 103859. https://www.sciencedirect.com/science/article/abs/pii/S014362282500356X

Turner, M. G. (1989). Landscape ecology: The effect of pattern on process. Annual Review of Ecology and Systematics, 20, 171–197.

Ibeabuchi Iro, S., & Chibuike Njoku, F. (2024). Analysis of Topographical Contribution of Flooding in Owerri Urban Imo State Using GIS And Remote Sensing Techniques. *African Journal of Social and Behavioural Sciences*, *14*(5). Retrieved from https://journals.aphriapub.com/index.php/AJSBS/article/view/2777

United Nations, Department of Economic and Social Affairs, Population Division. (2025). *World Urbanization Prospects: The 2025 Revision, Online Edition* [Data set]. https://population.un.org/wup/

Whitehand, J. W. R., Samuels, I., & Conzen, M. P. (2009). Conzen, M.R.G. 1960: Alnwick, Northumberland: a study in town-plan analysis. Institute of British Geographers Publication 27. London: George Philip. Progress in Human Geography, 33(6), 859-864. https://doi.org/10.1177/0309132509334948.